3

Mechanical and Thermal Properties

Everyday experience shows that polymeric materials display a remarkably wide range of mechanical behaviour, spanning brittle solid, rubber, leathery plastic, and strong fibre. Moreover, it is often evident that the mechanical character of a solid polymer is altered greatly by changes of temperature as small as a few degrees. In chapter 2 we saw that an amorphous polymer such as PMMA is brittle below its glass transition temperature T_g. At higher temperatures it softens progressively, turning gradually without any obvious discontinuity of property into a viscous liquid as the temperature rises.

We shall now consider how to describe this diversity of mechanical behaviour, paying particular attention to the sensitivity of mechanical properties to changes of temperature. This is a special characteristic of polymeric materials as a class, and one with important consequences for polymer processing and design.

3.1 Deformations: Stress and Strain

We apply the word *brittle* to a solid which will not support large deformations, and which fractures without appreciable yielding. If a specimen of such a material is stressed to failure in a tensile testing apparatus, the characteristic stress–strain relationship ideally resembles the curve shown in figure 3.1(a). It is clear that Hooke's law is obeyed, at least approximately

$$\epsilon = D\sigma \tag{3.1}$$

(D is called the *compliance*, the 'spring constant'); it is more usual in engineering contexts to express equation 3.1 with σ as the dependent variable:

$$\sigma = E\epsilon \tag{3.2}$$

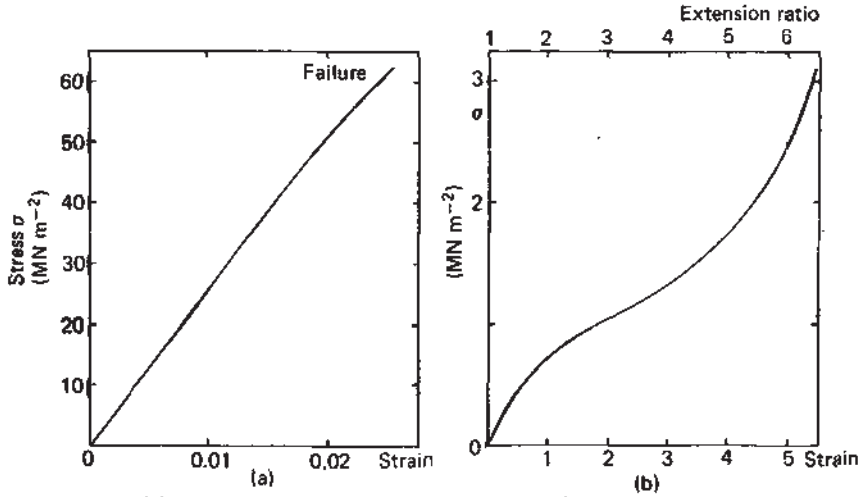

Figure 3.1 (a) Typical tensile stress–strain curve of a brittle polymer, such as PMMA or CA at a low temperature. (b) Typical tensile stress–strain curve for an unfilled rubber. Note that (a) and (b) have different stress and strain scales

where E is the tensile elastic modulus (Young's modulus). Such brittle behaviour in glassy polymers well below T_g is much the same in essence as the brittleness of many metals, inorganic glasses and ceramics. Failure occurs cleanly and suddenly, with no gross prefracture yield. At any strain below the failure strain the deformation is entirely reversible. Such behaviour is described as *elastic*. An elastic body spontaneously recovers its original state on removal of the applied stress, and the energy expended to produce the original deformation is totally recoverable.

3.2 Brittle Hookean Solids

Inability to support tensile strains greater than a few per cent indicates that there is little scope within the micro- or crystal structure for internal reorganisation of brittle solids in response to an imposed stress. The largeness of the elastic modulus reflects the large forces needed to move atoms even fractionally from their equilibrium positions by bond stretching, bond compression, or by a change of spacing between adjacent non-bonded atoms.

The calculation of the modulus depends on a detailed knowledge of the energies of interaction between all atoms in the solid. Although precise calculations may not be possible, it is interesting to note that for small strains there should be little difference between the behaviour in tension and compression. If the energy of interaction of a typical pair of neighbouring atoms is represented by the curve U (figure 3.2), then d^2U/dr^2 in the vicinity $U = U_0$

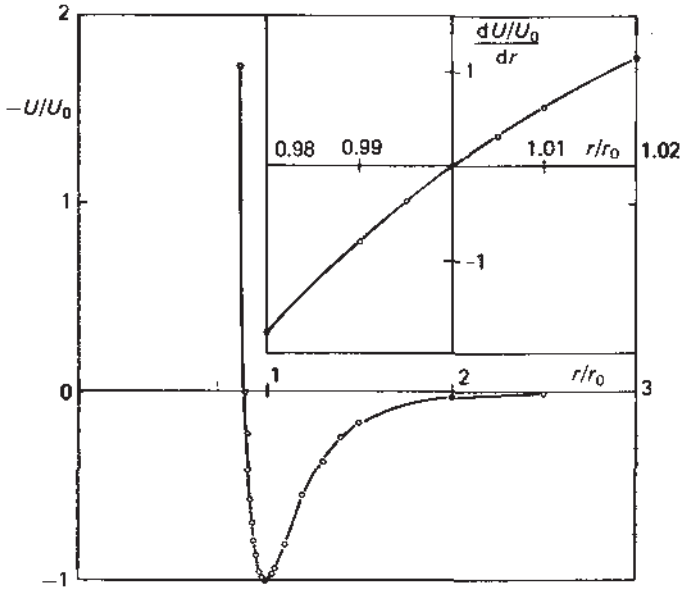

Figure 3.2 Energy of interaction $U(r)$ of non-bonded atoms or molecules calculated from the Mie equation $U = -a/r^m + b/r^n$ with $m = 6$ and $n = 12$ (van der Waals' interaction). U_0, r_0 are equilibrium energy and distance of separation. For many solid materials the bulk modulus K is proportional to $d^2U/dr^2|_{r_0} = nmU_0/r_0^2$. Inset shows dU/dr for small strains $\pm 0.02r_0$

represents the force/deformation ratio, which we may take as a rough measure of the modulus. For small deformations the force evidently depends approximately linearly on the deformation (thus Hooke's law) and is about the same in compression as in tension. In fact by Gruneisen's first rule the bulk modulus $K \approx nmU_0/9V_0$ where V_0 is the molar volume. If we consider the van der Waals' interaction between the CH_2 groups of neighbouring PE molecules we may take $U_0 = 8.0$ kJ/mol CH_2 and $V_0 = 22$ cm^3. Hence we obtain $K \approx 3 \times 10^3$ MN/m^2, in good agreement with the experimental value found for polycrystalline PE.

3.3 Elastic Moduli of Glassy Polymers

Table 3.1 lists the elastic moduli of a number of glassy polymers (at specified temperatures) and other engineering materials. The polymers are less stiff than structural metals and ceramics by one or two orders of magnitude. Where deformation involves primary bond stretching (as in metals, ionic solids, carbon fibre) moduli of 10^5–10^6 MN/m^2 are found. Small strains in glassy polymers

TABLE 3.1
Young's modulus E of polymers in the glassy state and of selected engineering materials

	E(MN m^{-2})
PMMA (−125 °C)	6.3×10^3
(25 °C)	3.3×10^3
PS (25 °C)	3.5×10^3
PC (25 °C)	2.3×10^3
PETP (25 °C)	2.0×10^3
LDPE (−50 °C)	1.8×10^3
Tungsten	4.1×10^5
Cast irons	$1.2–1.8 \times 10^5$
Copper	1.1×10^5
Aluminium	7×10^4
Diamond	9.5×10^5
Dense aluminium oxide	4×10^5
High modulus carbon fibre	4.2×10^5
Soda glass	6.9×10^4
Fused quartz	7.3×10^4

apparently involve relative movements of non-bonded atoms (van der Waals' force fields), which is reflected in lower elastic moduli, $10^3–10^4$ MN/m^2.

3.4 Rubber Elasticity

We have described the stress–strain diagram obtained in a tensile test on a brittle solid. A similar test carried out on a rubbery polymer or *elastomer*, however, yields a very different stress–strain curve – figure 3.1(b). Once again the behaviour is elastic, since the specimen returns to its original state ($\sigma = 0, \epsilon = 0$) on removal of the load. None the less, three differences stand out. First, Hooke's law is not obeyed. In particular the modulus increases at large strains. Second, relatively enormous deformations may be attained. Rubbers may be repeatedly extended to as much as five times their unstrained length completely reversibly. This represents a strain perhaps one thousand times greater than the failure strain of many brittle solids. Third, the mean elastic modulus is relatively very low (two or three orders of magnitude less than that of a glassy polymer).

In rubbery solids, molecular reorganisation in response to applied stress is

relatively easy, although ultimately restrained by a small concentration of crosslinks between chains. (In the rubbery state of nonelastomers such as PMMA and PS, permanent chemical crosslinks are absent and chain entanglements serve to restrain the relative movement of chains. Such materials only exhibit full elastic recovery in short-term experiments, because the entanglements free themselves over a sufficiently long period of time permitting irreversible movements of chains in the solid.)

In the unstrained state (state A of figure 3.3) the molecular chains adopt the most probable random arrangements consistent with chemical crosslinking or entanglement coupling. To a good approximation, the sections of the molecules which lie between each pair of crosslinks behave as freely jointed chains, and the spatial distribution of these chains within the rubber network corresponds to the maximum in the gaussian function already shown in figure 1.6(b). The state A is not static at the molecular level because of the thermal motion of the chains; however, the distribution averaged over the very large number of conformational arrangements which can be adopted is constant. When the rubber is deformed (A → B) the separations of adjacent tie points in the network are changed in a manner which depends on the macroscopic strain. The deformation entails a shift in the random conformations of the freely jointed chains to less probable distributions. When the stress is removed the rubber rapidly and spontaneously recovers its unstrained condition as the chains return to a state indistinguishable

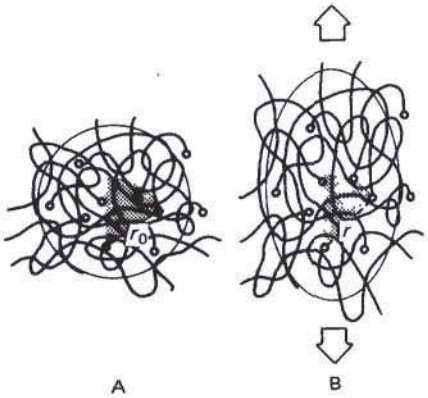

Figure 3.3 The rubbery state. A represents a small volume element of an unstrained material, B the same volume extended along the axis shown. Each line represents a chain segment between two tie points, depicted here as a free chain. The change $(r - r_0)$ in separation of adjacent tie points in each molecular chain depends on the angle θ (shown as a shaded sector). Averaged over the whole network $(r - r_0)$ is approximately proportional to the overall strain. (After Peterlin, A., 'Mechanisms of deformation in polymeric solids', *Polymeric Materials*, American Society of Metals, 1975, p. 181)

from A. The recovery from B to A occurs because random thermal motion tends to recreate the more probable distribution.

It is interesting to note that in compression (that is, bulk not uniaxial compression) the modulus of rubbery solids is much higher than in tension, similar in fact to that of other solids. This is so because the redistribution which occurs in extension and shear is no longer possible, and deformation can only occur by closer packing of molecules and compression of atom against atom.

This view of rubber elasticity provides the basis for a powerful statistical thermodynamic analysis of the rubbery state, which we may outline as follows. To transform state A to state B (figure 3.3) requires the expenditure of work because B has a higher free energy than A. We recall that the free energy is a composite quantity comprising enthalpy and entropy contributions. In elastomers, enthalpy differences between states like A and B are relatively small. Indeed an *ideal elastomer* is defined as one whose enthalpy is independent of strain (compare this with an ideal gas, whose enthalpy is independent of volume). In an ideal elastomer therefore the free energy difference between A and B (and hence the work necessary to deform the material) depends on the entropy difference between A and B, ΔS. ΔS can be calculated from the probability function $\omega(r)$ describing the distribution of chain conformations, since S = constant x ln $\omega(r)$. In turn the work of deformation = $-T\Delta S$, where T is the absolute temperature. This suggests that the work required to attain a particular strain increases as the temperature increases. The implications that the tensile modulus of a rubber should increase with temperature and that a rubber in tension should contract on heating are both borne out by experiment. Another interesting result of this analysis, also confirmed experimentally, is that rubbers become hotter during adiabatic stretching and cool on retraction. Real rubbers approximate to a greater or less extent to ideal elastomers.

3.5 Viscoelasticity

We have now described two types of mechanical response in polymers (the responses of the glassy state and the rubbery state) which are approximately elastic. We have noted that amorphous polymers exhibit both types of behaviour (figure 3.4). The glassy state occurs at temperatures well below T_g and the rubbery state somewhat above T_g. Between the two is a *transition zone*, usually spanning some 20 °C, in which the stiffness decreases rapidly with increasing temperature. In lightly crosslinked polymers (elastomers such as vulcanised rubbers) the rubbery state persists up to the highest temperatures at which the material is thermally stable. In non-crosslinked amorphous polymers (such as PMMA and PS) the rubbery state extends only to the vicinity of another transition temperature (or terminal zone) above which the polymer melts and is essentially fluid.

The mechanical behaviour of crystalline polymers is also greatly influenced

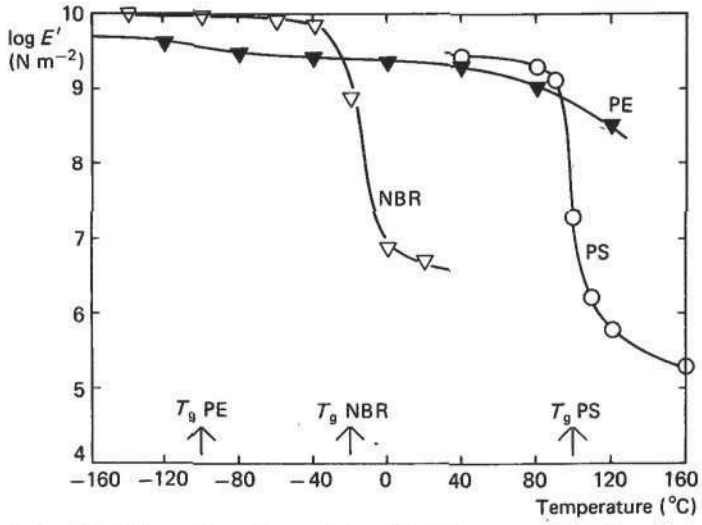

Figure 3.4 Variation of tensile modulus E' with temperature for a crystalline polymer HDPE and two amorphous polymers PS and NBR (an elastomer). The glass transition temperatures T_g are shown. PS is normally used at temperatures below its T_g and NBR above

by temperature (figure 3.4). The reduction in stiffness as the temperature rises is less pronounced than in amorphous polymers and the transition zone associated with T_g is generally broadened. The effect of crystallinity is to produce a leathery rather than a rubbery condition in the polymer above T_g. At still higher temperatures a reasonably well-defined melting temperature marks the appearance of the fluid state.

Figure 3.4 emphasises how sensitive to temperature is the mechanical behaviour of a polymeric material. At the lowest temperatures polymers, whether amorphous or crystalline, are brittle, approximately elastic, glasslike solids. At the highest temperatures uncrosslinked materials are molten, viscous substances, in which the response to an applied stress is flow. In the whole of the intermediate region, comprising the transition zone associated with T_g, the rubbery plateau, the leathery state of crystalline polymers, and the terminal zone, the mechanical behaviour shows features of both elastic solid and viscous liquid. Since the working temperatures of many engineering polymers fall in this intermediate region we must sometimes consider polymer solids as a class as *viscoelastic* rather than elastic bodies. The occurrence of viscous processes introduces time-dependence and sometimes irreversibility into the stress–strain behaviour of the polymeric materials. The central theme of polymer mechanics is the interrelationship of the variables stress, strain, time and temperature. In order to present a unified analysis of such varied mechanical behaviour it is useful to look again at the elastic response.

3.6 Elastic Solids: Stress–Strain Relations as Input–Output Functions

If the tensile test on an elastic solid is carried out at a uniform rate of straining, from zero to some terminal strain ϵ_1 below the point of fracture, the increments of strain produce simultaneous increments of stress (we say that stress and strain change *synchronously*), as shown in figure 3.5(a).

Alternatively, if a change in stress (say from zero to σ) is imposed instantaneously at t_1 (a step function of stress) the tensile strain response is immediate, ϵ rising to the constant value ϵ_1. The compliance D is therefore also a constant. If σ returns to zero at t_2 then ϵ returns also to zero at t_2, without any lag.

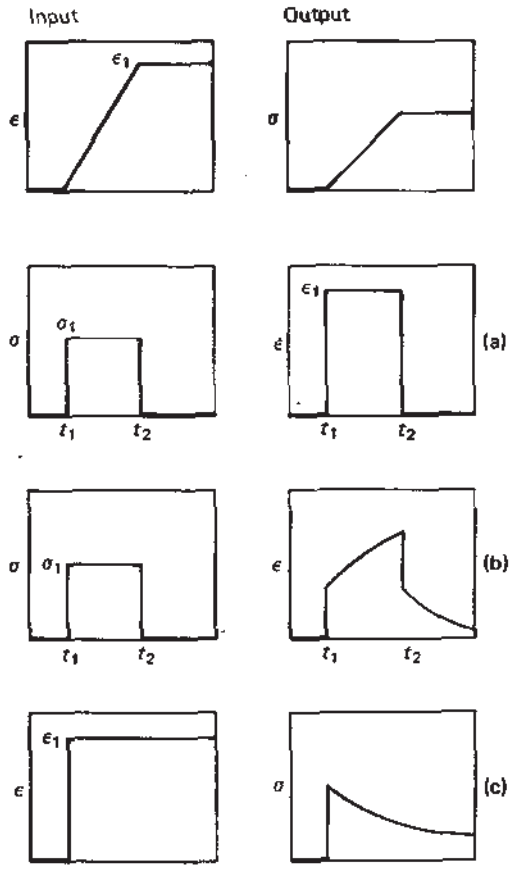

Figure 3.5 (a) Synchronous stress–strain behaviour in an elastic material. (b) Creep, recovery and (c) stress relaxation in a viscoelastic material

3.7 Viscoelastic Materials

Amorphous polymers above T_g do not show this behaviour. For example, the response to a step function of stress may be of the general form shown in figure 3.5(b). Now D is no longer a constant. For the interval t_1 to t_2, σ has a constant value σ_1 but ϵ is a function of time $\epsilon(t)$, thus

$$D(t) = \epsilon(t)/\sigma_1 \tag{3.3}$$

The form of figure 3.5(b) shows that the material continues to deform under constant load. This behaviour, known as *creep*, is in striking contrast to that of the elastic solid which deforms only while the load is being applied. Creep behaviour (to which we return in section 3.9) has some of the characteristics of liquid viscous flow, and time-dependent stress–strain relations of this general kind are thus described as *viscoelastic*. It is important to note that equation 3.3 describes *linear* time-dependent behaviour, i.e. ϵ and D are linearly related through the stress σ. If $D(t)$ is determined at one value of σ then the complete strain response can be calculated at any other stress. Such behaviour is often observed in amorphous polymers for small strains and short times. We return briefly in section 3.15 to the more general case of nonlinear viscoelasticity.

It is an important feature of linear viscoelasticity theory that the effects of a number of imposed stresses are additive. This is embodied in the *Boltzmann superposition principle*. It is of great practical importance since it means that the response of the material to a complicated stress (or strain) input function can be calculated from a quite small amount of data.

3.8 Stress Relaxation

An experiment to determine the creep response of a material imposes a stress (normally a constant load) and examines the time-dependent strain response of the specimen. If on the other hand a fixed strain ϵ_1 is imposed on the specimen, the measured stress is now time dependent – figure 3.5(c). The material exhibits a decreasing stress or *stress relaxation*, which for a linear viscoelastic body leads naturally to the definition of a stress relaxation modulus

$$E(t) = \sigma(t)/\epsilon_1 \tag{3.4}$$

(compare this with equation 3.3).

Can we be more precise in describing how *viscoelasticity* combines the properties of the elastic solid and the viscous liquid? A very useful method of analysis lies in the construction (on paper only!) of ideal mechanical models which simulate the stress–strain–time behaviour of the real materials. The mechanical models are normally built up from only two kinds of unit: the hookean spring $\epsilon = D\sigma$ and the linear viscous element (usually represented by a dashpot, a perforated piston moving in a cylinder filled with a viscous fluid) for which

$d\epsilon/dt = \eta^{-1}\sigma$, where η is the viscosity. A series combination of spring and dashpot is known as a *Maxwell element* and a parallel combination is called a *Voigt element*. The response of the Maxwell element to a constant stress is

$$\epsilon = (D + t/\eta)\sigma \tag{3.5}$$

ϵ increases linearly with time – figure 3.6(a). Similarly the response to a step function of strain is

$$\sigma = \epsilon \exp(-t/\eta D)/D \tag{3.6}$$

Thus the stress relaxes exponentially as shown in figure 3.6(b); the rate of relaxation is determined by the characteristic time ηD. A long slow relaxation (with a long relaxation time) is caused either by a weak spring constant or a high viscosity. The underlying linearity of the system is revealed by the fact that the relaxation time depends only on D and η.

In the Voigt element the parallel combination prevents the development of creep at a constant rate under a constant load

$$\epsilon = \sigma D[1 - \exp(-t/\eta D)] \tag{3.7}$$

As $t \to \infty$, $\epsilon \to \epsilon_\infty = \sigma D$

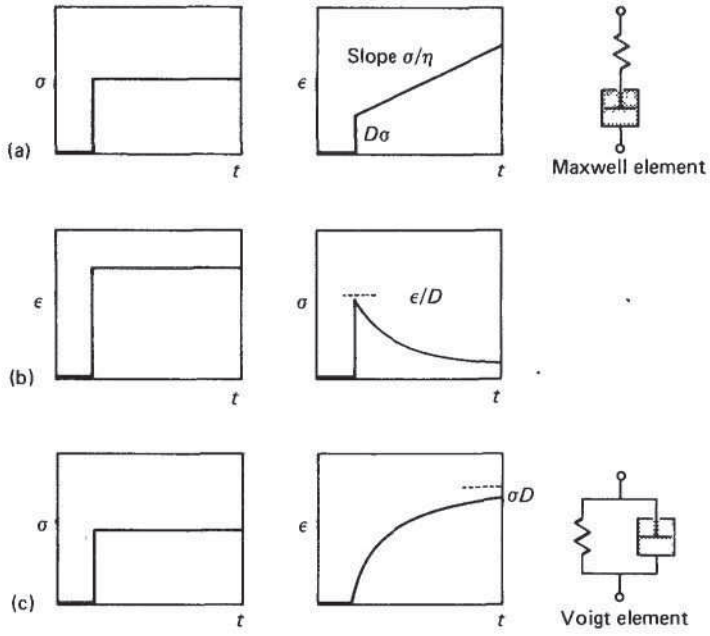

Figure 3.6 Maxwell and Voigt elements. (a) Maxwell element: step function of stress and strain response. (b) Maxwell element: step function of strain and stress response. (c) Voigt element: step function of stress and strain response

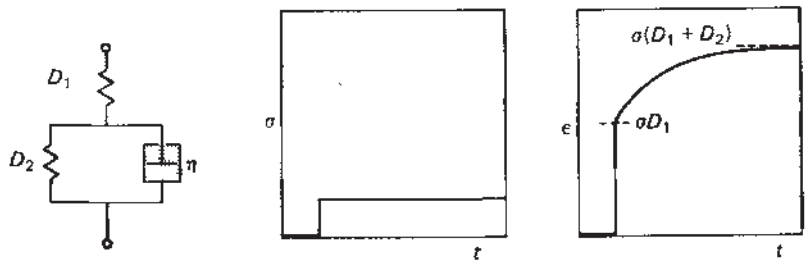

Figure 3.7 Creep compliance of a three-element model. Strain response to a step function of stress of spring, series-coupled to a Voigt element (a form of the standard linear solid)

This ultimate strain ϵ_∞ is the same as the strain developed in an elastic material of compliance D in the absence of a dashpot. The essential difference is that the strain response is not instantaneous but *retarded*. The quantity ηD is here the characteristic *retardation time* of the system. (To impose a step change of strain on a Voigt element is unrealistic as it implies an infinite instantaneous stress in the dashpot.)

More complex responses can be obtained by adding further units in series or parallel with Maxwell or Voigt elements. An important three-element model is shown in figure 3.7.

It is important to remember that such model descriptions of viscoelastic behaviour are highly simplified representations of the mechanics of polymer solids. Nevertheless there is some physical justification for combining reversible, elastic and irreversible, dissipative elements in this way. The merit of these models is in providing a basis for developing differential equations for $\sigma(t)$ and $\epsilon(t)$, which may later be generalised.

3.9 Creep and Stress Relaxation Experiments

The step input functions of stress and strain which we have just examined are of special interest because they correspond to two of the principal experimental arrangements in common use in testing the mechanical properties of plastics. These are the creep test and the stress relaxation test in uniaxial tension. Creep tests may also be carried out in flexure and in torsion. The response to a constant rate of strain may also be conveniently studied with conventional tensile testing machines. The response of the Maxwell, Voigt or three-element model to a constant imposed strain rate can readily be obtained.

Creep tests are particularly simple in concept, although careful design of apparatus is essential if high accuracy is to be attained in tests which may last for many months. The deformation of the specimen has been measured by a

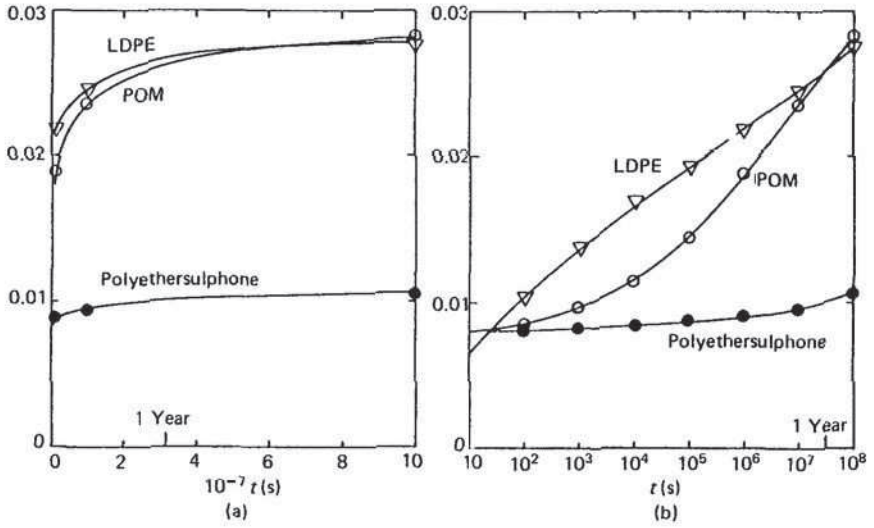

Figure 3.8 Tensile creep at 20 °C of LDPE (20 MN m^{-2}), POM copolymer (20 MN m^{-2}) and polyethersulphone (2 MN m^{-2}) (a) Strain plotted against time. (b) Strain plotted against log(time). (Data from ICI Ltd)

variety of mechanical, electromechanical and optical devices. Figure 3.8 shows the strain–time curves for three thermoplastics. It is clear that the behaviour of the thermoplastics somewhat resembles that of a Maxwell element: an instantaneous deformation followed by creep. However, if the creep strain is followed for long times it is frequently found to increase at a reducing rate. The creep rate of the Maxwell element on the other hand is constant and to that extent the Maxwell element is too simple a model. The three-element model is a significant improvement and shows an exponentially falling creep rate; moreover, complete strain recovery eventually follows removal of stress. The typical rubbery solid shows a retarded elastic response similar to that of a Voigt element. The strain–time curve of the Voigt element under constant stress is a simple exponential. This is not the case for real rubbers.

3.10 Empirical Creep Equations

Our discussion of the creep response of the Maxwell three-element model suggests that it should be possible to split the observed creep strains of polymeric materials into two parts

$$\epsilon = \epsilon_1 + \epsilon_2(t) \tag{3.8}$$

Here ϵ_1 is the instantaneous elastic strain and ϵ_2 is a time-dependent strain.

Although ϵ_2 does not in fact depend linearly or exponentially or in any other simple way on t it is often possible to find an *empirical* function which fits the observed data well

$$\epsilon - \epsilon_1 = \sigma f(t) \tag{3.9}$$

where σ is the stress. Knowledge of $f(t)$ then permits computation of ϵ at any time and any stress. Conversely a large body of creep data may be condensed into a single function f. For example, the creep of several thermoplastics at low stress may be represented approximately by the empirical function

$$\epsilon = \sigma(B + At^{\alpha})$$

or

$$(\epsilon - \sigma B)/\sigma = At^{\alpha} = f(t) \tag{3.10}$$

For such materials the creep curve is usefully displayed on a logarithmic or semi-logarithmic plot (*see* figure 3.8(b), LDPE and polyethersulphone); at corresponding times the creep strain is proportional to the stress (linear behaviour).

3.11 Dynamic Response

We have seen how the characteristic relaxation time or retardation time arises in response to simple input functions. These interesting results suggest that we should look next at the response to *periodic* driving functions. For example, what is the stress response of the Maxwell element to a sinusoidal strain? Intuitively we feel that the answer depends on the relative magnitudes of the period of the imposed strain cycle and the relaxation time of the element. In the case of an extremely slow sinusoidal strain, almost total relaxation of the stress occurs at every point on the cycle. The material behaves like a viscous fluid. Any vestigial stress response is almost exactly out of phase with the driving function, since the stress is at its greatest when $d\epsilon/dt$ is at a maximum, that is, when $\epsilon = 0$. If on the other hand the cyclic strain rate is very rapid the dashpot is unable to respond to any extent. The viscous response is entirely prevented and the stress unrelaxed. The amplitude of the induced periodic stress is at a maximum. The material behaves as a purely elastic body. At intermediate frequencies, the stress response is diminished in amplitude and lags in phase. This dynamic viscoelastic behaviour is expressed most succinctly by defining a complex strain

$$\epsilon^* = \epsilon_0 \exp(i\omega t) \tag{3.11}$$

and a complex stress $\sigma^* = \sigma_0 \exp(i\omega t + i\delta)$, where δ is the phase angle between strain and stress. The complex compliance

$$D^* = D' - iD'' = \epsilon^*/\sigma^* = \epsilon_0 \exp(-i\delta)/\sigma_0 \tag{3.12}$$

For a Maxwell element the total rate of strain is simply the sum of the spring and dashpot rates of strain

$$\frac{d\epsilon^*}{dt} = D\frac{d\sigma^*}{dt} + \eta^{-1}\sigma^* \tag{3.13}$$

Here D is the compliance of the spring. By substituting and separating real and imaginary parts we obtain

$$\epsilon_0/\sigma_0 = D\cos\delta + \eta^{-1}\omega^{-1}\sin\delta \tag{3.14}$$

and

$$\tan\delta = 1/\eta\omega D = D''/D' \tag{3.15}$$

By definition (equation 3.12) $D' = \epsilon_0 \cos\delta/\sigma_0$ and thus from equations 3.11 and 3.13 it follows that $D' = D$.

Similarly $D'' = \epsilon_0 \sin\delta/\sigma_0 = 1/\eta\omega$. σ_0, the amplitude of the stress response at any frequency ω, is given by

$$\sigma_0 = \epsilon_0/(D\cos\delta + \sin\delta \times \eta^{-1}\omega^{-1}) \tag{3.16}$$

At high frequencies $\delta \to 0$ and $\sigma_0 = \epsilon_0/D$. At very low frequencies $\delta \to \pi/2$ and $\sigma_0 = 0$. When $\omega = 1/\eta D$ $\tan\delta = 1$ and $\sigma_0 = \sqrt{2}\epsilon_0/2D$.

Figure 3.9 shows ϵ and σ for the frequencies $\omega = 10^n/\eta D$, $n = -1, 0, 1$.

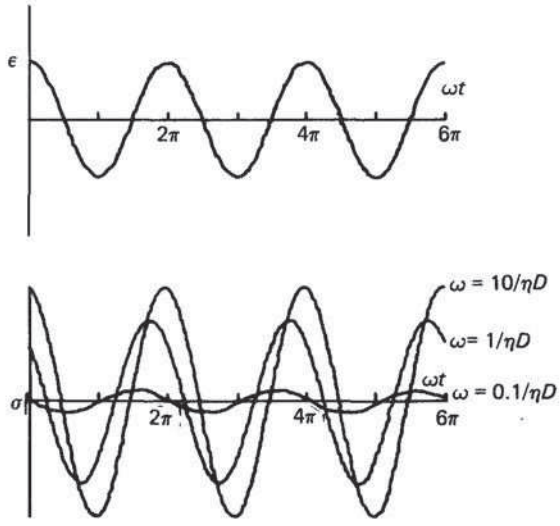

Figure 3.9 Stress response of a Maxwell element to a sinusoidal strain at three different frequencies (*see* equations 3.15 and 3.16). Note the reduction in stress amplitude and the increase in phase angle as frequency falls

The three-element model shown in figure 3.7 has properties resembling those of polymer materials. At high frequencies the parallel combination of spring (compliance D_2) and dashpot behaves as a rigid link, and the system behaves as though it consisted only of the series spring (compliance D_1). At very low frequencies the system reduces to a series combination of springs (compliance $D_1 + D_2$). In general at any frequency ω

$$D' = D_1 + \frac{D_2}{1 + \omega^2\tau^2}$$

and

$$D'' = \frac{D_2\omega\tau}{1 + \omega^2\tau^2}$$

where

$$\tau = D_2\eta \tag{3.17}$$

When

$$D_2\eta\omega \gg 1 \quad D' = D_1$$

When

$$D_2\eta\omega \ll 1 \quad D' = D_1 + D_2$$

When

$$\omega = \tau^{-1} \quad D' = D_1 + D_2/2$$

(figure 3.10). The response of real polymer materials can be accurately modelled only by assuming an extended array of Voigt elements, and a corresponding

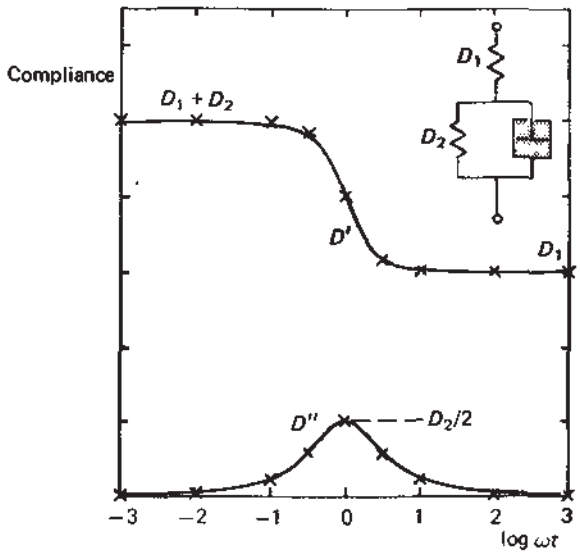

Figure 3.10 Frequency dependence of the storage compliance D' and the loss compliance D'' (components of the complex compliance D^*) calculated for the standard linear solid (arbitrary values $D_1 = 3$ and $D_2 = 2$ are used)

distribution of retardation times τ. This has the effect of broadening the loss peak.

Model analysis (and the generalised compliance D) may be used to represent several kinds of deformation in real solid materials. Shear deformation (involving only changes of shape) and bulk compression (involving only changes of volume) are the fundamental modes. The corresponding compliances are

J = Shear strain/Shear stress

B = −(Bulk strain/Pressure)

Other deformations may be decomposed into combinations of these two. Thus simple extension in response to a uniaxial tensile stress produces both shape and volume changes. The tensile compliance $D = J/3 + B/9$.

Finally we note that the equations developed above may be expressed in terms of modulus rather than compliance. Just as $D = 1/E$ (equations 3.1 and 3.2), so $D^* = 1/E^*$, where E^* is a complex modulus $E^* = E' + iE''$. Once again real solids have distinct shear and compressional moduli, $G^* = 1/J^*$ and $K^* = 1/B^*$, respectively. Most interest in polymer viscoelasticity lies in the mechanics of shear deformation, studied either directly in pure shear or indirectly in extension.

3.12 Energy of Deformation

We turn now to a new consideration. A force acting on a material and producing a deformation performs work. This work is $\int \sigma \, d\epsilon$ per unit volume, where σ is the instantaneous stress and ϵ the strain. The integral represents the energy required to produce deformation. What becomes of this energy of deformation?

In the case of a hookean spring, the energy of deformation is stored indefinitely in the spring and may be completely recovered by allowing the spring to act on another load and return to zero strain. In contrast, the energy of deformation expended on a dashpot is at once converted irrecoverably to heat. The amount of work performed by the load in producing a given displacement in the dashpot depends on the rate of displacement $r = d\epsilon/dt$.

$$\text{Work performed} = \text{Load} \times \text{Displacement}$$

$$= \eta r \times \epsilon$$

The work expended in producing a strain against viscous forces can be made as small as desired by reducing the rate of displacement.

If the load is cyclic then

$$\text{work performed per cycle} = \oint \sigma \frac{d\epsilon}{dt} \, dt$$

$$= \oint \sigma_0 \cos \omega t \, \frac{\sigma_0 \cos \omega t}{\eta} \, dt$$

$$= \pi \sigma_0^2 / \eta \omega \qquad (3.18)$$

$$\text{Power required} = \frac{\pi\sigma_0^2}{\eta\omega}\frac{\omega}{2\pi} = \frac{\sigma_0^2}{2\eta} \tag{3.19}$$

However, as the frequency ω increases, the strain amplitude produced by a given σ_0 decreases. If the spring and dashpot are series coupled to give a Maxwell element, then the energy of deformation is stored at high frequencies and lost at low frequencies. In the three-element model, the energy of deformation is stored at both high and low frequencies and partially lost at intermediate frequencies only. The maximum loss occurs when tan δ and D'' reach their maximal values. It is for this reason that tan δ is often described as the *loss tangent*. The lost energy appears as heat which may produce large increases in temperature in a material subject to continuous cyclic stress at frequencies near to τ^{-1}. In contrast, the energy of *elastic* deformation is zero over a complete cycle.

3.13 Anelastic Mechanical Spectra

A simple device for studying mechanical loss is the torsional pendulum, shown in figure 3.11(a). The decay of the amplitude of the torsional oscillations is exponential: the cyclic strain damped by viscoelastic loss in the polymer rod or thread may be written

$$\epsilon = \epsilon_0 \exp(-\alpha t) \sin(\omega t - \delta) \tag{3.20}$$

and

$$\tan\delta = 2\alpha/\omega = \Lambda/\pi \tag{3.21}$$

where Λ is the *logarithmic decrement* $\ln(\epsilon_i/\epsilon_{i+1})$ calculated from the amplitude of successive oscillations – figure 3.11(b).

The frequency of oscillation is determined by the moment of inertia of the disc and may in practice be varied between 0.1 and 10 Hz. It is common to study the dependence of tan δ on temperature at a fixed frequency. Such a plot is known as an anelastic spectrum or loss spectrum – figure 3.11(c). The analysis of the three-element model leads us to expect maxima in tan δ when ω^{-1} is equal to a characteristic relaxation time of the material. Polymer materials invariably show a number of loss peaks, and we identify each one with one of the types of molecular motion described in chapter 2. The relaxation times of each decrease with increasing temperature, so that there is for each at any frequency a maximum in the associated loss process at a characteristic temperature. Alternatively loss spectra can be obtained by studying forced vibrations over a wide range of frequencies at a fixed temperature. Such equipment is of particular value in studying the technical performance of rubbers where the dynamic response to forced vibrations of 100–1000 Hz is of interest.

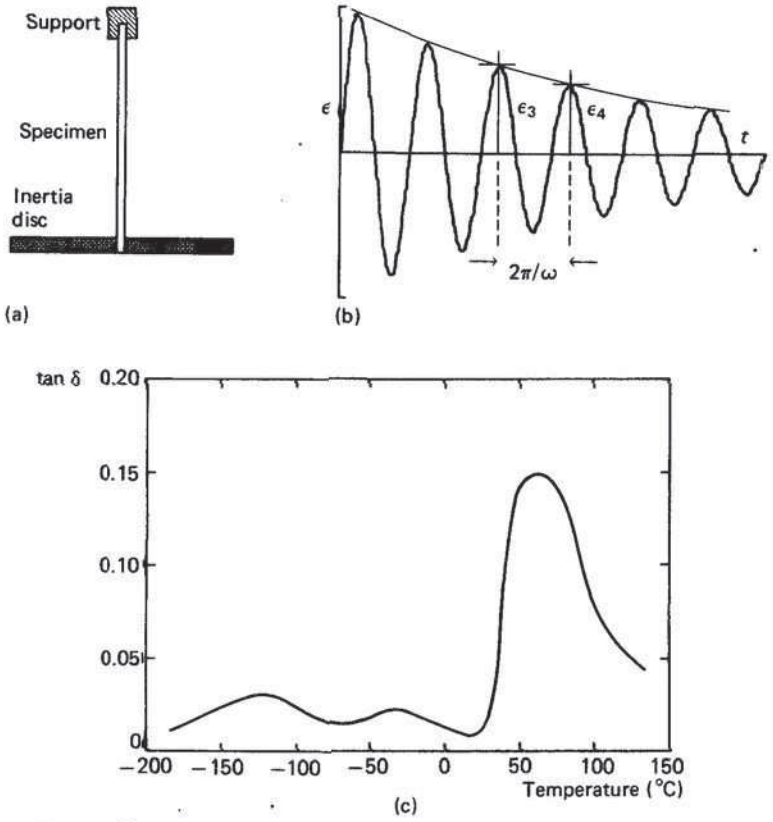

Figure 3.11 (a) Simple torsional pendulum for the study of viscoelastic loss. (b) Damped sinusoidal strain showing exponential decay of strain amplitude from which logarithmic decrement and loss tangent may be calculated. (c) Anelastic spectrum of PA 6

3.14 Time–Temperature Correspondence and the WLF Equation

We consider next how the time (or frequency) dependence of modulus or compliance variables is related to the temperature dependence. Figure 3.12 shows shear stress relaxation modulus data for an amorphous polymer at two temperatures T_0 and T_1. The two curves clearly have some similarity of shape and it is found that they are in fact reducible to a single curve by the application of a dimensionless scaling factor a_T to the time axis. Thus

$$G(t,T_0) \approx G(t/a_T, T_1) \tag{3.22}$$

a_T, as the subscript indicates, depends on the temperatures T_1 and T_2. This amounts to saying that stress relaxation modulus curves obtained at different

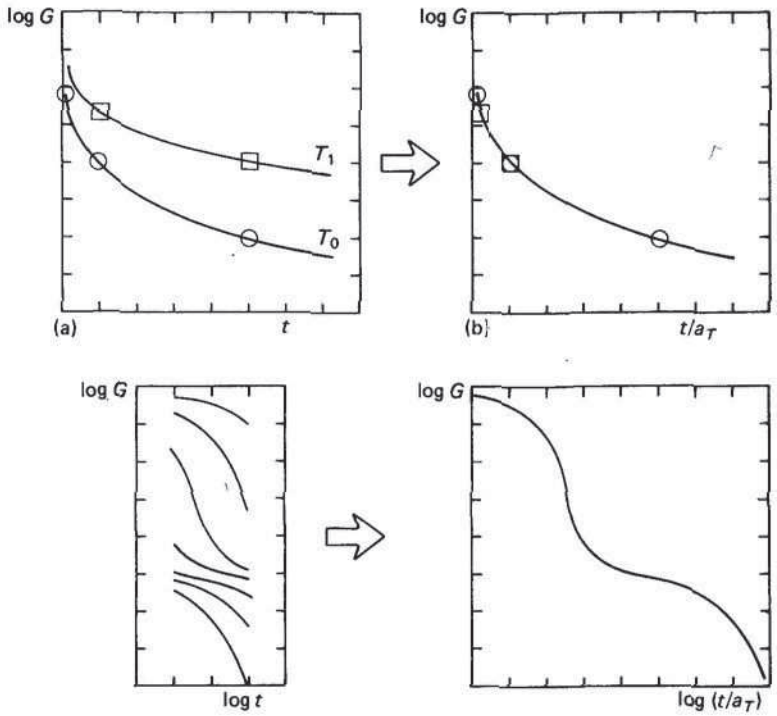

Figure 3.12 Stress relaxation modulus $G(t)$ of an amorphous polymer at two temperatures. The curves have similar shapes and can be made to lie on a common curve by the application of a suitable scaling factor a_T to the time axis. (b) Formation of a stress relaxation master curve

temperatures lie on a common master curve when plotted against the reduced variable t/a_T. The position of the master curve on the t/a_T axis depends on the choice of an arbitrary reference temperature T_0 for which $a_T = 1$. If a logarithmic time axis is used, the scale factor a_T becomes a horizontal shift $\log a_T$ (*see also* figure 3.12). A minor correction is normally applied to allow for effects arising from changes in density ρ. A reduced relaxation modulus $G^r = T_0\rho_0\, G(t, T)/T\rho$ is plotted against t/a_T rather than $G(t, T)$ itself. This method of reduced variables can also be applied to small strain creep compliance data by plotting $JT_0\rho_0/T\rho$ against t/a_T. Dynamic compliance and modulus data are obtained as functions of the frequency ω; in these cases ωa_T is the appropriate reduced variable.

These ideas form the basis of the concept of *time–temperature correspondence*. This has been a very fruitful approach to the analysis of data in polymer viscoelasticity because it enables us to separate the time and temperature dependences of important mechanical variables. The time

dependence is given by a master curve at one reference temperature and the temperature dependence by a function $a_T(T)$. $a_T(T)$ may be found empirically, simply by selecting that value of a_T at each temperature which gives the most satisfactory smooth master curve. This procedure has already been illustrated in figure 3.12. One notable feature of the master curve is that it can span many decades of time (or frequency). Thus we can obtain valuable information about extremely short-time or extremely long-time mechanical properties at a temperature of interest by experiments over a limited span of time (or frequency) at several other temperatures. This adds greatly to the usefulness of a number of experimental techniques.

The importance of time–temperature correspondence was further enhanced by the discovery of Williams, Landel and Ferry that for amorphous polymers in the transition zone and the rubbery state the empirically determined shift factors $\log a_T$ could be closely fitted to the expression

$$\log a_T = -C_1(T - T_0)/(C_2 + T - T_0) \tag{3.23}$$

Furthermore if the glass transition temperature T_g is taken as the reference temperature we obtain the usual form of the *WLF equation*

$$\log a_T^{T_g} = -C_1^{T_g}(T - T_g)/(C_2^{T_g} + T - T_g) \tag{3.24}$$

This equation was originally established empirically, but its form has since been derived from theoretical models of molecular motion in solids. $C_1^{T_g}$ and $C_2^{T_g}$ are found to be approximately constant for a wide range of different polymers. Further discussion of the WLF equation can be found in the texts listed at the end of this chapter.

The molecular basis of time–temperature correspondence may be broadly described as follows. The viscoelastic response of a polymer solid depends on the rates of a variety of molecular motions. The effect of change of temperature is to alter these rates. The implication of time–temperature correspondence is that the various molecular motions controlling the viscoelastic properties *all have the same temperature dependence.* Although not generally true, this assumption appears to be widely valid for amorphous polymers in the transition zone, the rubbery state and the terminal zone.

3.15 Nonlinear Viscoelastic Materials

In earlier sections of this chapter we have made much use of the compliance D, as defined in equation 3.3. The compliance is essentially a parameter of *linear* viscoelasticity theory, as its definition implies that the general strain response

$$\epsilon = f(\sigma, t) \tag{3.25}$$

may be written

$$\epsilon = \sigma D(t) \tag{3.26}$$

which expresses a linear relation between ϵ and σ.

Practical polymers may often be treated as linear viscoelastic materials for relatively small deformations and short times. We have already seen how a creep compliance may be fitted to an empirical linear expression. However, strictly linear behaviour is not generally observed. Figure 3.13 shows creep curves for PP. It can be seen that replotting the data in the form $\epsilon(\sigma, t)/\sigma$ does not yield a single master curve. Under these circumstances, analytical avenues do not lead anywhere very useful, and test results such as creep data must be given in graphical or tabular form. The *isochronous stress–strain curve* is a particularly useful form of presentation which shows the relation between σ and ϵ at some fixed time t. A family of such curves is often displayed on a single graph. The isochronous stress–strain curve of a linear viscoelastic material is itself linear, and so the curvature of lines such as those shown in figure 3.14 is a measure of the nonlinearity of the viscoelastic behaviour of the material. Alternatively the *isometric stress–time curve* may be constructed (figure 3.14).

As an alternative to graphical methods a more elaborate empirical equation may be used, such as that of Findley

$$\epsilon(\sigma, t) = \epsilon_0 \sinh(a\sigma) + bt^n \sinh(c\sigma) \tag{3.27}$$

3.16 Impact Performance

Impact damage is a common kind of failure in plastic components, but impact performance is one of the most difficult of mechanical properties to assess

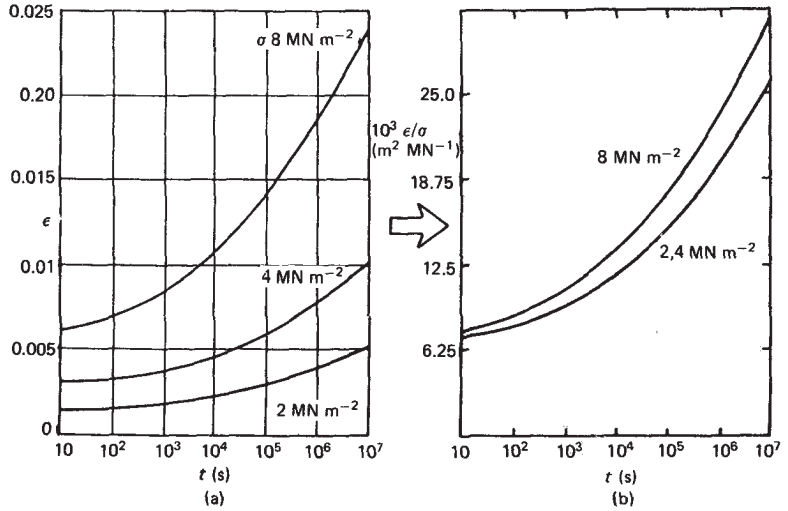

Figure 3.13 (a) Creep curves of PP at 20 °C at three stresses σ. (b) The same data replotted as creep compliance $D = \epsilon(t)/\sigma$ showing that the creep strain does not depend linearly on stress at the two highest values of σ

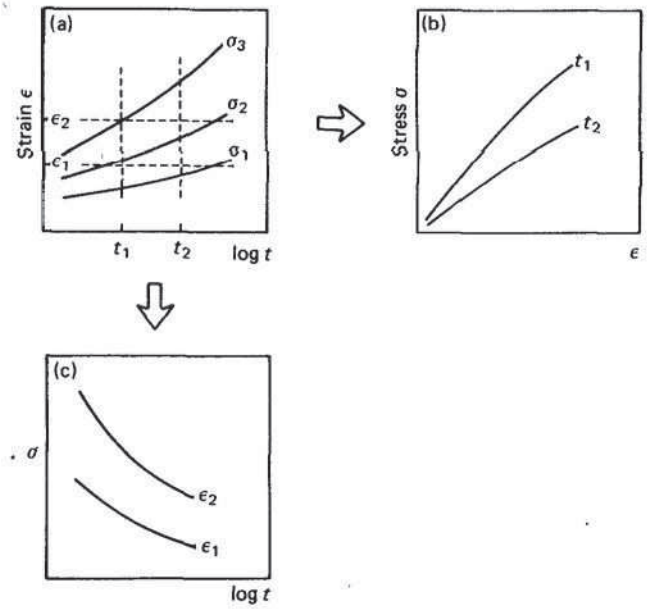

Figure 3.14 Derivation of isochronous stress–strain curves (b) and isometric stress–time curves (c) from a family of creep curves (a)

satisfactorily. It is impracticable to simulate the wide variety of impacts to which an article may be subject in its service life. Many impact test devices have been used, some involving falling balls and darts. The most important impact test machines, however, are of the pendulum type, similar in principle to those used in the testing of metals. Pendulum testers are classified as *Charpy type* or *Izod type*, depending on the way in which the rectangular test piece is held (figure 3.15). In both cases the test piece is normally notched.

The pendulum strikes the test piece at the lowest point of its swing. In failing the test piece takes energy from the down-swinging pendulum, reducing the amplitude of its next upward swing. This amplitude is recorded. The loss in energy of the pendulum is a measure of the *impact strength* (IS) of the material. It is usual to quote the impact strength as *energy to break/fractured area.* It should be noted that the term impact strength is a misnomer, as the word 'strength' usually has the meaning of a critical stress. However, the usage is firmly established in work on impact.

It is found that the impact performance depends greatly on the characteristics of the notch. For example, in tests with blunt notches (tip radius $r = 2$ mm) PVC has a higher impact strength than ABS. If the test pieces are prepared with sharp notches ($r = 0.25$ mm) the order is reversed, and ABS is found to have the higher impact strength – figure 3.16(a). Test results depend also on crack depth

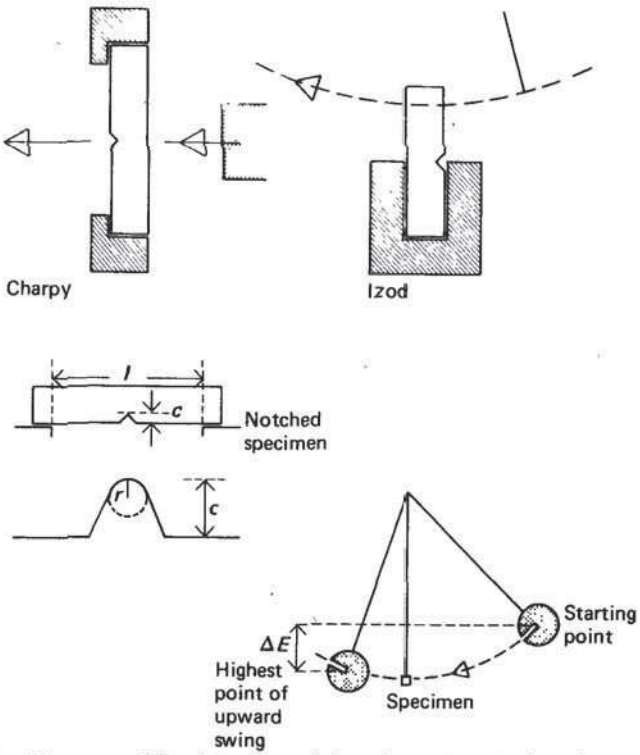

Figure 3.15 Charpy and Izod type pendulum impact tests, showing notching and mounting of the specimen

(c) and for some materials the effects of both c and r on impact strength can be expressed through a simple stress concentration factor $1 + 2(c/r)^{1/2}$ (*see* p. 77). However, the variety of types of impact failure observed, even in a standard Charpy test, is considerable, ranging from brittle failure without any yielding to ductile failure with many intermediate cases. For many design purposes it is satisfactory to rank materials according to a three-fold classification at 20 °C (*see* table 3.2). Impact strength of course may depend strongly on temperature – figure 3.16(b). An arbitrary brittleness temperature T_B is sometimes defined as the temperature at which IS (r = 0.25 mm) equals 10 kJ/m^2.

Other factors such as molar mass, presence of additives and processing conditions may influence impact strength. An interesting example is the way that water content affects the impact strength of polyamides (nylons). It is well known that nylons absorb several per cent by weight of water when immersed or conditioned in a humid atmosphere. At room temperature dry nylon is notch brittle with an IS (r = 0.25 mm) of about 4 kJ/m^2; wet nylon has an impact strength greater than 20 kJ/m^2 and is classified as tough.

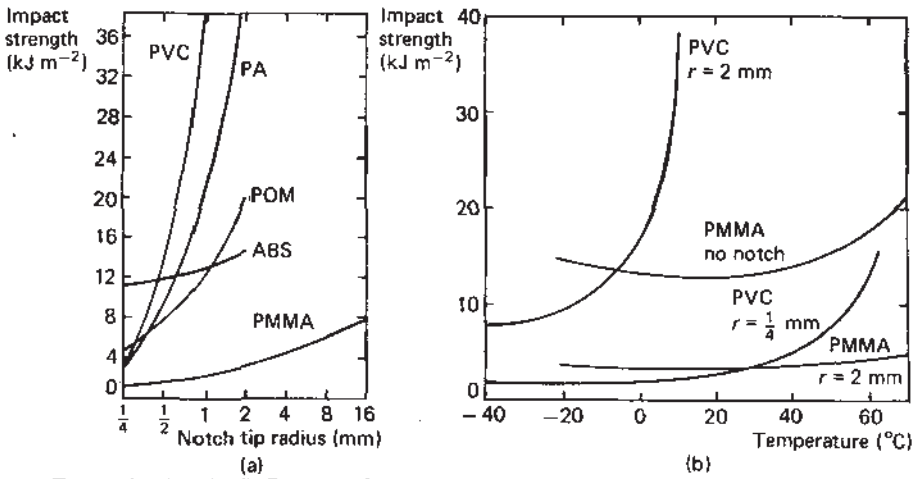

Figure 3.16 (a) Influence of notch tip radius on the impact strength of five polymers. (b) Influence of temperature on the impact strengths of polymers (after Vincent)

TABLE 3.2
Three-fold classification of Charpy impact performance of polymers (20 °C), after Vincent

Brittle	*Notch brittle*	*Tough*
Acrylics	PP	Wet nylon
Polymethylpentene	Cellulosics	LDPE
Glass-filled nylon	PVC	ABS (some)
PS and HIPS	Dry nylon	PC (some)
	Acetals	PTFE
	Polysulphone	Some high
	Toughened acrylics	impact PPs
	HDPE	
	PPO	
	ABS (some)	
	PC (some)	
	PETP	

Notes:
Brittle – specimens break even when unnotched.
Notch brittle – specimens do not break unnotched, but break when sharp-notched (r = 0.25 mm).
Tough – specimens do not break completely even when sharp-notched (r = 0.25 mm).

3.17 Yield and Fracture

By the criteria of the previous paragraphs, a tough polymer is one which has a high energy to break in an impact test and which fails in a ductile manner. A traditional metallurgical approach to toughness is through the stress–strain relation. The toughness of a metal is measured by the area beneath its stress–strain curve taken to failure. Toughness is associated with ductility, and both the continuum mechanics and the micromechanics of plasticity in metals are now well understood. The search for improved impact performance has more recently stimulated a similar systematic study of yield and fracture processes in polymers. Yield phenomena are exploited in polymer technology in such operations as fibre-drawing and cold-forming (*see* chapter 6), adding further to the significance of basic research in this subject.

In general a polymer may show either brittle or ductile behaviour in a mechanical test according to circumstances. The main controlling factors are the time scale and the configuration of the test procedure, and the temperature. Low rates of straining and high temperatures favour a ductile response – figure 3.17(a, b, c). The Charpy impact method is effectively a high speed test of

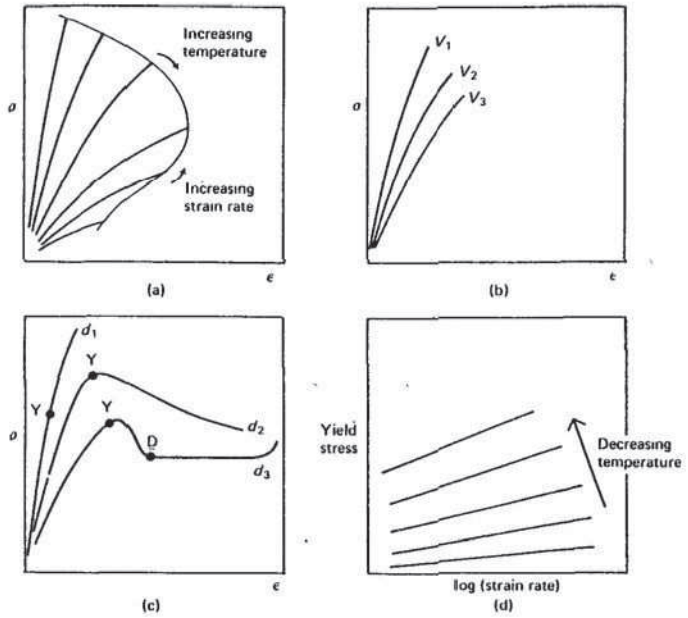

Figure 3.17 (a) Failure envelope showing effect of straining rate and temperature on the stress–strain curve of polymers. (b) Influence of straining rate on tensile strength of a brittle polymer ($V_1 > V_2 > V_3$). (c) Types of ductile behaviour in polymers. (d) Influence of testing speed on the tensile yield stress of an amorphous polymer at several temperatures.

failure in flexure. At the other extreme of time scale are high load creep tests continued to failure. The conventional tensile test may be carried out over a wide range of fixed straining rates. We have already described the characteristics of brittle failure under tensile stress in section 3.1; the material fails at relatively low strain with little or no yield. The *tensile strength* is the nominal stress at failure; for polymers this is not a single-valued property of the material at each temperature since it depends on the rate of straining.

In the case of ductile behaviour the stress–strain curve takes one of the several forms represented by d_1, d_2 and d_3 in figure 3.17(c). In d_1, a decrease in slope at Y marks a more or less well-defined yield point which is followed by uniform yielding until failure. In d_2 a maximum in the nominal stress develops at Y leading to the formation of an unstable neck. As the specimen is further extended it continues to yield inhomogeneously at the neck until failure occurs. In d_3 the formation of a neck at Y is followed by strain-hardening which stabilises the neck. This is the type of inhomogeneous yield behaviour which gives rise to drawing. Extension of the specimen beyond D occurs by increasing the length of the necked portion at constant cross-section (figure 3.18). This proceeds until a limiting overall strain or *natural draw ratio* is attained, after which the fully drawn polymer moves up the final part of the curve to failure.

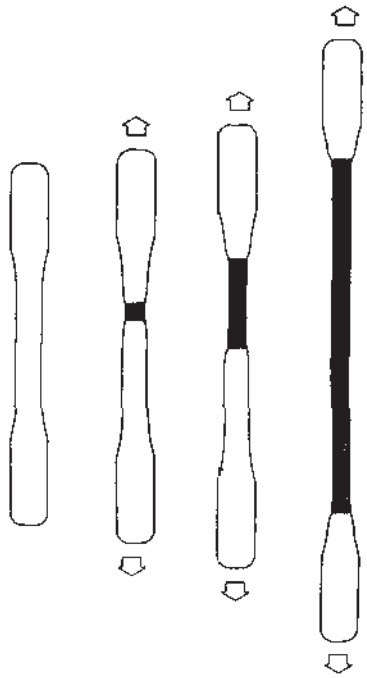

Figure 3.18 Ductile behaviour in a cold-drawing polymer

At temperatures far below T_g polymers show brittle behaviour. In any particular test a ductile–brittle transition may be observed at a temperature T_b (not the same as the impact brittleness temperature T_B). T_b is well below T_g. Between T_b and T_g the yield stress σ_Y falls with rising temperature and approaches zero in the vicinity of T_g itself.

Studies of yield stress in metals have confirmed the general validity of the von Mises yield criterion, according to which yielding occurs when the total shear strain energy reaches a critical value. In metals yield stress is approximately independent of hydrostatic pressure which produces dilatational strain only. In polymers the yield stress increases with hydrostatic pressure. The von Mises yield criterion therefore requires modification for polymeric materials. Both shear and hydrostatic stresses exist in uniaxial tension and compression and in flexure so that observed yield stresses are found to be dependent on the test configuration. One important method of presenting long-term strength data is by means of high load creep curves or the creep failure stress curves derived from such creep tests (figure 3.19).

In this brief discussion of yielding we have so far considered only the macroscopic or continuum features of plasticity. However, the occurrence of ductile behaviour in glassy polymers below T_g must be considered somewhat unexpected from a molecular point of view. How do glassy polymers deform to large strains without fracture at temperatures at which large-scale molecular motion is normally non-existent? This question is not yet finally resolved. The influence of hydrostatic pressure on yield stress once again directs attention to the free volume; at high tensile stresses the hydrostatic tension component may cause the free volume to increase and permit segmental motion in the solid. T_g itself is known to rise with increasing hydrostatic pressure. The stress field itself may assist viscous flow processes by favouring conformations which extend chains in the direction of the applied stress. A model of the morphological changes accompanying fibre-drawing in crystalline polymers has already been described in chapter 2.

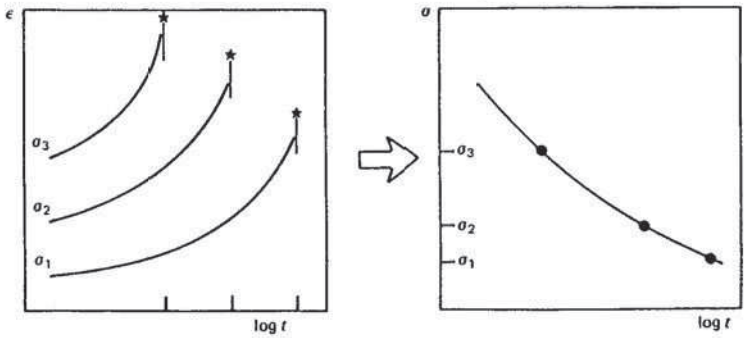

Figure 3.19 Creep failure stress–time curve derived from a family of creep failure curves. * marks the time of failure (rupture) on the creep curves

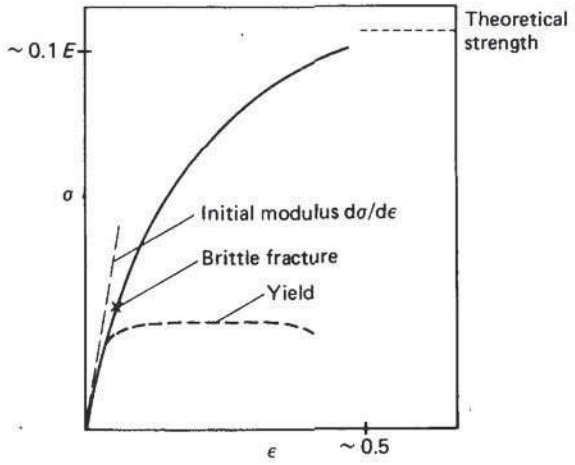

Figure 3.20 Limitation of strength of materials imposed by yield and fracture processes. Simple models of ideal solids predict theoretical strengths of $\sim 0.1E$ and failure strains of 0.2–0.5

Yield and fracture are of great practical interest for two reasons. For engineers it is the occurrence of these processes which set limit states for design: critical stresses and strains which must not be exceeded in performance. To materials scientists yield and fracture are processes which generally prevent materials attaining anything approaching their theoretical strengths. As we have already pointed out in figure 3.2 the small strain elastic modulus of a solid material is determined by the interatomic force field. Real materials generally show initial moduli not very different from the theoretical predictions. However, these same materials usually fail to attain the theoretical strengths calculated from the bond energies either because plastic deformation intervenes prematurely or because brittle fracture occurs to limit the attainable stresses (figure 3.20).

Modern brittle fracture theory has grown largely out of the ideas of Griffith, originally proposed around 1920 to account for the observed breaking strengths of glass fibres. Griffith theory has subsequently been applied widely to fracture phenomena in both non-metallic and metallic materials. Detailed accounts will be found in general materials science texts; here we describe briefly its central ideas in the context of glassy polymers.

Griffith supposed that the tensile strengths (and failure strains) of brittle materials fell far short of theoretical expectations because the materials are generally not truly homogeneous. The real brittle solid is spectacularly weakened by *flaws* of various kinds which lead to local irregularities in the lines of stress (figure 3.21). If the flaw takes the form of a crack transverse to the direction of the stress σ, stress concentrations σ_c develop at the ends a, a′ of the crack.

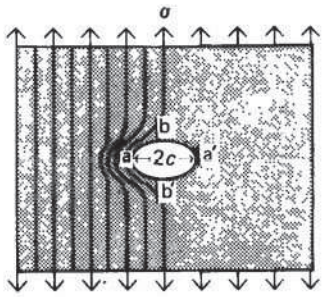

Figure 3.21 Stress concentration at the ends a and a' of an elliptical crack in a uniformly stressed plate. Stress is reduced in the vicinity of b and b'; the net reduction in strain energy in a plate of unit thickness due to the presence of the flaw $\Delta_1 = \pi c^2\sigma^2/E$. The flaw extends spontaneously if $d\Delta_1/dc \geqslant d\Delta_2/dc$, where Δ_2 is the surface work of fracture (*see* text)

Griffith made use of the equations previously established by Inglis for the stress concentration about an elliptical hole in a uniformly loaded plate. The stress concentration factor $2(c/r)^{1/2}$ associated with a long microcrack of very small radius r at the tip can clearly be very large. If σ_c is sufficiently great to cause local failure then the crack propagates and brittle fracture ensues. Next we ask: what determines the critical value of σ_c? Griffith expressed the criterion of crack propagation in terms of energy and argued that the crack advances only if the strain energy released in extending the crack equals or exceeds the energy required to form the new fracture surfaces. The presence of the crack reduces the total strain energy by an amount Δ_1. Δ_1 may be calculated from the distribution of stress about the crack (figure 3.21): thus

$$\Delta_1 = \pi c^2\sigma^2/E \tag{3.28}$$

If Δ_2 is controlled by the specific surface energy γ of the solid

$$\Delta_2 = 4c\gamma \tag{3.29}$$

Therefore

$$\sigma_f = (2E\gamma/\pi c)^{1/2} \tag{3.30}$$

is the critical fracture stress. From breaking strength data it appears that, for glass, Δ_2 is indeed largely determined by γ. For metals and glassy polymers, on the other hand, the formation of new fracture surface involves processes of plastic deformation in the region of the advancing crack tip. Thus the quantity Δ_2 represents a generalised surface work term, which embraces all those processes involved in crack extension. Likewise γ is interpreted as a generalised *fracture surface energy.*

What of the cracks or flaws themselves? In general, brittle fracture may arise from stress concentrations either associated with holes or notches deliberately formed in the material or associated with natural flaws present in the

microstructure. In glass, the natural flaws which initiate fracture are usually surface scratches. If these are absent very high tensile strengths can be achieved. Similar exceptional strengths can be attained in ceramic whiskers and fibres of high structural perfection. In metals, the flaws naturally present may arise from the movement of dislocations. What is the nature of the flaws in glassy polymers? Under many circumstances a deliberately introduced crack in a glassy polymer propagates by the formation of a *craze* which runs ahead of the crack tip. The craze material comprises fibrils and microvoids in approximately equal volumes. Crazing is a characteristic form of microyielding associated with brittle fracture. Craze lines are easily observed by the scattering of light from refractive index discontinuities produced by the microvoids. Brittle fracture in materials free of deliberate cracks may proceed by the formation at one or more microscopic inhomogeneities (including voids and inclusions) of craze material, followed by rupture, followed by propagation of the initiated crack. Craze lines are formed at right angles to the stress in glassy polymers such as PS under high uniaxial tensile stress as a prelude to brittle fracture.

A large body of experimental and theoretical work now exists on the fracture mechanics of polymers. The generalised $E\gamma$ of equation 3.30 is designated K, the stress intensity factor. The critical value of K, K_c, is therefore a measure of the fracture toughness of the material, an intrinsic material property. The quantity $G_c = K_c^2/E$, the strain energy release rate (per unit area of fracture, not per unit time) is an essentially equivalent measure of material fracture toughness. These quantities are usually measured in controlled crack growth experiments. Data for some polymers are collected in table 3.3. The traditional Izod and Charpy impact tests (*see* figure 3.15 and text) have been analysed in terms of linear fracture mechanics theory, with the result that it is now possible to derive K_c (or G_c) data from such tests, provided that the notch depth can be varied. The energy absorbed on impact $\Delta E = G_c \times bd\phi$, where b is the width of the sample, d the thickness and ϕ is a geometrical factor depending on c/d.

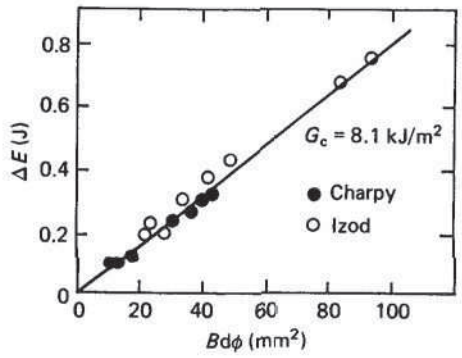

Figure 3.22 Charpy and Izod impact test data for medium density polyethylene at 20 °C (after Williams)

TABLE 3.3
Izod fracture toughness G_c (kJ/m) (after Williams)

Polystyrene	0.8
Poly(methyl methacrylate)	1.4
Poly(vinyl chloride)	1.4
HDPE	3.1
Polycarbonate	4.8
Polyamide PA-66	5.0
PE (rel density 0.94)	8.4
High impact polystyrene	14
LDPE	34
ABS	47

Plotting ΔE against $bd\phi$ for various values of c allows G_c to be calculated (figure 3.22).

3.18 Friction of Polymers

Friction and wear characteristics are important but complicated aspects of the mechanics of polymers. Knowledge of both is fundamental to the design of rubber vehicle tyres, but the general significance of friction and wear has widened as many other polymers have found engineering application as moving parts. Frictional forces developed between the moving fibres in textile manufacturing processes have also been much studied. The whole subject is a complex one, lacking firmly established quantitative theories.

The classical engineering laws of sliding friction are simple. Amontons' laws state that the friction F between a body and a plane surface is proportional to the total load L and independent of the area of contact A. The friction of a moving body is normally somewhat less than that of a static body. The kinetic friction is considered to be independent of velocity. The *coefficient of friction* μ is defined as the ratio F/L. Both materials (slider and surface) must be specified. Coefficients of friction for a number of materials are given in table 3.3. Polymers as a class exhibit a wide range of friction properties. PTFE is particularly used for its remarkably low friction, whereas rubbers possess high values of μ.

Amontons' laws hold only approximately for metals and frequently do not hold for polymers. The facts can be explained only in terms of microscopic surface features of the solids. First we accept that the surfaces of materials are not atomically flat but microscopically irregular. Therefore the true area of contact between two surfaces is very much less than the apparent area of contact, and the entire normal force is carried by the tips of the asperities. At these contact points the local stress is so great that severe deformation occurs, and the

TABLE 3.4
Coefficients of friction

	μ_k *coefficient of sliding friction*
PTFE	0.04–0.15
LDPE	0.30–0.80
HDPE	0.08–0.20
PP	0.67
PS	0.33–0.5
PMMA	0.25–0.50
PETP	0.20–0.30
PA 66	0.15–0.40
PVC	0.20–0.90
PVDC	0.68–1.80
PVF	0.10–0.30
SBR	0.5–3.0
BR	0.4–1.5
NR	0.5–3.0

Typical reported values; sliding on various countersurfaces

tip of each asperity is crushed to produce a small plane or almost plane region. Over this small region intimate atomic contact exists between the two surfaces and *adhesion* occurs (van der Waals' forces or stronger chemical forces act across the contact faces). In order to move the body across the surface it is now necessary either to break the adhesional bonds at the interface AA′ (figure 3.23) or to shear one or other of the materials at some plane (BB′ or CC′) very near the surface. These ideas lead to a basic concept of adhesional friction: that the friction $F = As$, where A is the true area of contact and s is the shear strength of the material. To the extent that soft materials are weak and hard materials strong, the effects of factor A and s are in opposition (figure 3.23). This is why such diverse engineering materials as metals, ceramics and polymers may have surprisingly similar coefficients of friction.

In the case of metals the true area of contact produced by *plastic* deformation of surface asperities is roughly proportional to the load, so that the first law holds. Generally this law does not hold for polymers. First, for rubbers the deformation is largely elastic rather than plastic and the area of contact increases with $L^{2/3}$ rather than L. Thus the coefficient of friction decreases with

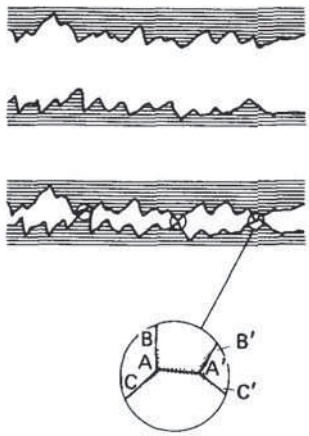

Figure 3.23 Micromechanics of friction: adhesional contact occurs at the asperities and sliding motion requires shearing at or near the interface

pressure. Second, for polymers which deform viscoelastically the friction obeys a law of the form

$$F = kL^x$$

or

$$\mu = kL^{x-1} \tag{3.31}$$

with $\frac{2}{3} < x < 1$. For example x has the value 0.85 for PTFE over 10 orders of magnitude in L.

The shearing processes dissipate energy to an extent that depends on the viscoelastic properties of the material, and hence depends on both the temperature and the strain rate. Figure 3.24 shows that the coefficient of friction of crystalline polymers above T_g depends strongly on the sliding speed, and passes through a maximum. These curves are shifted to the right as the temperature rises. Grosch showed that similar effects are observed in rubbers sliding on smooth glass surfaces, and he demonstrated the viscoelastic origin of the friction by showing that the WLF shift (*see* section 3.14) condenses the data into a single friction–temperature–velocity master curve (figure 3.24). Furthermore, the positions of the peak in the friction master curve and the peak in the loss tangent master curve for each rubber were such that the ratio $V/2\pi\omega$ is about 6 nm, pointing directly to the molecular scale of the energy absorption process.

If two materials of very different hardness are sliding against each other the adhesional model of friction is incomplete. This situation is common in polymer applications where polymer materials bear on metal surfaces. The asperities of the harder material plough into the surface of the softer, producing grooves which may recover as the ploughing tip moves on or from which material may be

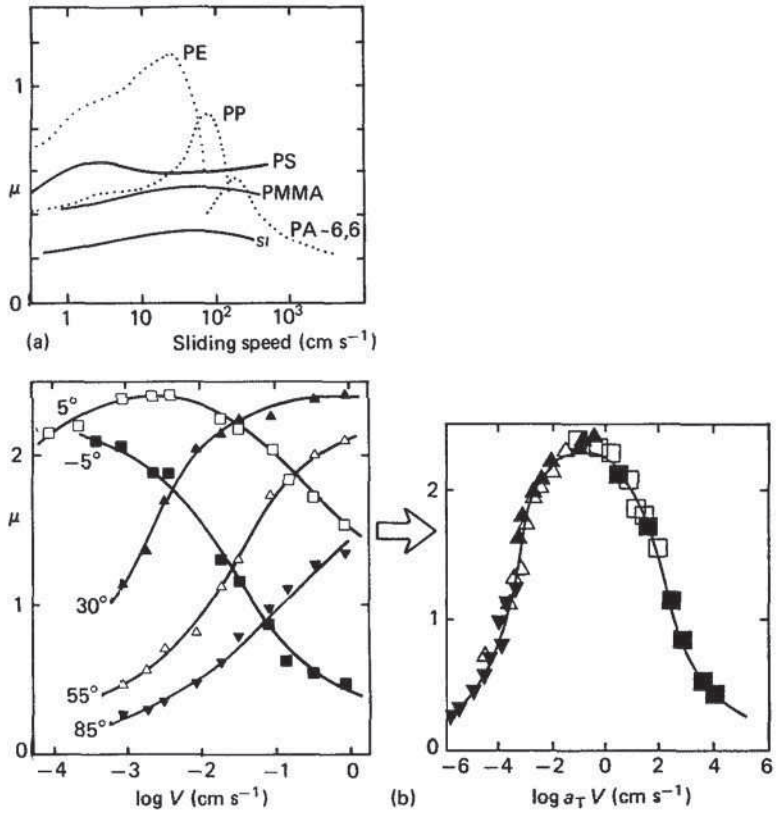

Figure 3.24 (a) The coefficient of friction μ of six polymers, showing dependence on sliding speed at room temperature (after McLaren and Tabor). (b) Coefficient of friction of acrylonitrile–butadiene elastomer on wavy glass as a function of sliding speed V at several temperatures; and master curve obtained by application of WLF shift (after Grosch)

torn out completely. In either case energy is absorbed by the deformed surface and partially dissipated through viscoelastic loss. There are both adhesional and deformational contributions to the energy of sliding one surface across another, and hence to the friction. We thus have two processes absorbing energy and producing friction, and both are expected to be sensitive to strain rate and temperature.

PTFE has an exceptionally low coefficient of friction ($\mu = 0.06$). This material is apparently able to form only weak adhesional bonds (cf. section 6.7), but this fact alone seems an inadequate explanation. HDPE has a coefficient of friction ($\mu = 0.08$) almost as low as that of PTFE, whereas LDPE shows a value of ~0.3. Furthermore, for both PTFE and HDPE μ rises to ~0.3 at higher sliding speeds. It is probable that some unusual mode of shearing occurs at the

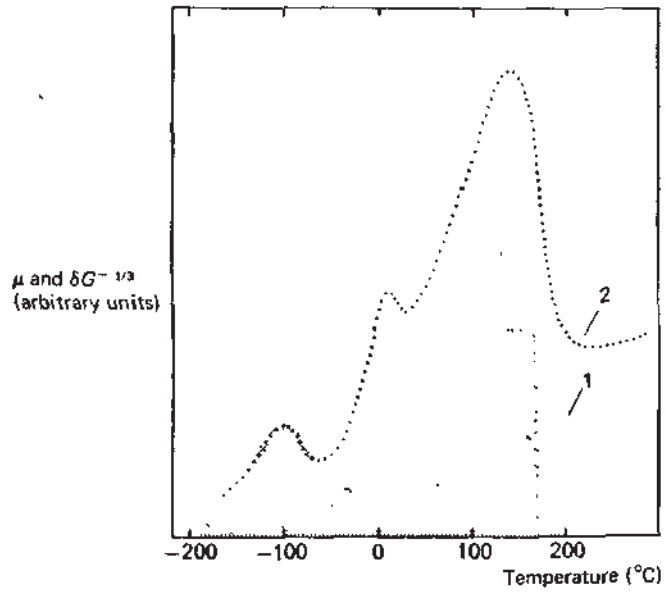

Figure 3.25 Temperature dependence of rolling friction and of hysteresis loss of PTFE compared. Curve 1 (shaded): the quantity $\delta G^{-1/3}$ measures the mechanical energy loss per cycle (δ is the loss angle and G the torsional modulus) Curve 2 (dotted): μ the coefficient of friction (After Ludema and Tabor)

polymer surface during sliding, and that this can occur because of the regular and unbranched molecular structure.

Rolling friction is determined largely by deformational energy losses since the tensile strength (rather than the shear strength) of the adhesion in the contact regions is low. A correlation is usually found between the coefficient of rolling friction and other viscoelastic properties (*see* figure 3.25). Rolling friction has much in common with lubricated sliding for in this case the thin liquid film of lubricant between the surfaces provides a plane of extremely low shear strength, and once again deformational processes dominate the friction. The observed coefficient of friction of rubbers depends on the loss: high loss rubbers show higher coefficients of friction than low loss rubbers of the same hardness in both rolling and lubricated sliding. In consequence high loss rubbers have been used to improve the skid resistance of motor vehicle tyres.

3.19 Wear

Both the shearing of adhesive bonds and the ploughing of deformations may remove material from the surface of the softer material. Wear and friction are

thus closely related and are really two aspects of the same set of phenomena. In addition fatigue in the surface layers may cause material to become detached. Although wear characteristics are of great technical and commercial significance the processes are complex and knowledge is largely empirical. The history of attempts to evaluate the wearing properties of flooring materials illustrates the difficulties of devising simulation tests. Abrasion resistance and related wear characteristics are in practice assessed by numerous *ad hoc* test procedures, specific to particular industries and technologies.

The amount of material removed from a surface by wear in the course of its sliding a distance D generally increases as the load L increases. If we measure the loss of material by the volume V of material removed then we may define the *abrasion factor* $A' = V/DL$. The abradability $\gamma = A'/\mu$, where μ is the coefficient of friction. Because of the close relation between wear and friction it is not surprising that γ is found to depend on the sliding speed and temperature. Wear is ultimately controlled by the deformation and failure behaviour of the polymer.

The observed wear characteristics emerge from a most complex interplay of elementary mechanical processes. The wearing forces produce extreme local strains. These strains are created and released at a variety of strain rates because of the microscopic but somewhat random scale of the events. Frictional heating introduces large local changes in temperature, which may markedly alter the viscoelastic response of the material. Finally, the phenomena are controlled by the nature of the *surfaces* of the materials, which frequently differ from the bulk solid.

Despite these difficulties the ideas summarised here give considerable insight into the nature of wear and abrasion. They are of great value in unifying the results of diverse technical tests, suggesting correlations between experimental parameters and rationalising test results. Wear, like metallic corrosion and the degradation of polymers by weathering processes, is immensely wasteful of materials and human effort. Its study forms part of the science of tribology (and more generally of terotechnology).

3.20 Heat Transmission

Innumerable engineering uses of polymers involve the transmission of heat. In some cases this is an incidental effect, as when rubber vehicle tyres become hot by viscoelastic loss. In other situations the control of heat flow is a primary consideration. For example polymer materials are used as thermal insulants in many industries. In every case the design engineer must consider the working temperatures reached within these materials. We have seen earlier how sensitive are the mechanical properties of polymers to changes of temperature. We shall see in chapter 5 that excessive heating can cause serious irreversible deterioration of polymers through chemical degradation processes. The thermal properties discussed here also have an important bearing on the fire behaviour of polymers.

The methods of analysis of heat flow are much the same whatever the nature of the material and depend on a knowledge of two material properties, the thermal conductivity λ and the specific heat capacity (or specific heat) c_p.

The heat flow q at any point in a solid is proportional to the temperature gradient

$$q = -\lambda \frac{d\theta}{dx}$$

Thus if the surfaces of a slab are maintained at temperatures θ_1 and θ_2 then the *steady* heat flow is

$$q = \lambda a(\theta_1 - \theta_2)/d$$

where a is the slab area and d the thickness. For a series of similar slabs of different materials the rates at which heat is transmitted are proportional to the thermal conductivities.

If we consider transient rather than steady flows then rates of change of temperature within the solid are determined by the quantity

$$\alpha = \lambda/c_p\rho$$

rather than λ alone. α is the *thermal diffusivity*. How quickly the temperature rises when heat flows into a material at a particular rate depends inversely on ρc_p, the heat capacity of unit volume. We shall discuss first λ and then briefly c_p.

3.21 Thermal Conductivity

At atomic level the effect of applying heat at one face of a cold slab is to increase the amplitude of thermal vibration in that face. This additional thermal energy then diffuses in the direction of the opposite face at a rate which for non-metals depends on how strongly the vibrational motion of adjacent atoms and groups is coupled. Strong coupling occurs in covalently bonded materials and transmission of heat is relatively efficient in ordered crystalline lattices. Thus, materials such as crystalline silica (quartz) and diamond, in which all atoms are built into the crystal structure by strong covalencies, are good thermal conductors. This is particularly so at low temperatures where such materials compare with metals in thermal conductivity. As the temperature rises, the thermal motion of the lattice offers increasing resistance to the flow of heat and λ falls. Resistance to the flow of heat also arises from defects in the crystal structure. An extreme of disorder is reached in amorphous solids, which show characteristically low thermal conductivities (compare crystalline and amorphous silica in figure 3.26). Molecular solids in which secondary chemical forces bind the crystal structure together conduct heat poorly because of the weak coupling between molecules. Elementary solid state theory shows that $\lambda = c_p(\rho K)^{1/2} l$ where

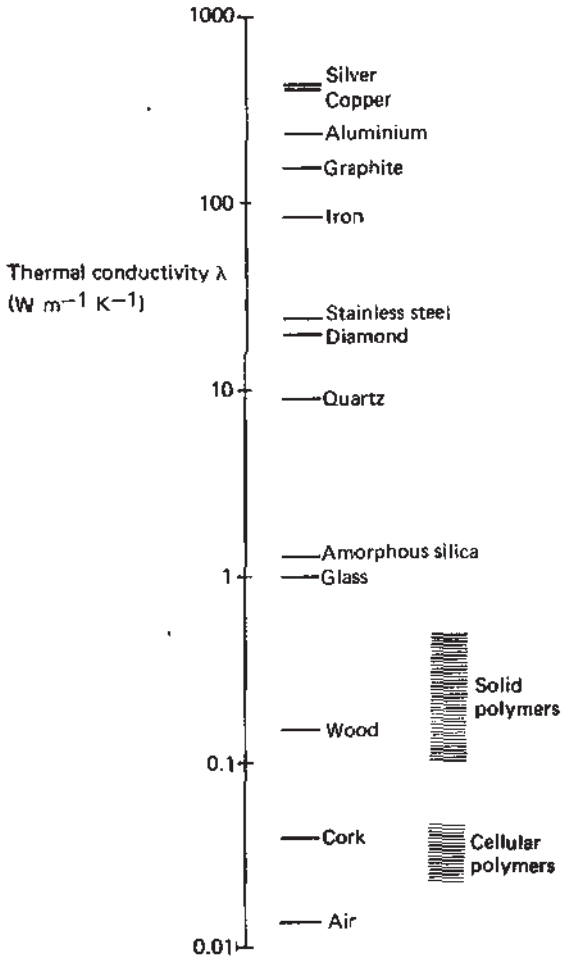

Figure 3.26 Thermal conductivity λ of selected materials

K is the elastic bulk modulus and l the mean free path of the thermal vibrations (phonons). For polymers taking $K \approx 10^3$ MN m^{-2} and $l \approx 200$ pm (the separation of adjacent polymer chains) we obtain $\lambda \approx 0.3$ W m^{-1} K^{-1}, in broad agreement with observed values.

In the case of metals at normal working temperatures the contribution of atomic lattice motion to the thermal conductivity is masked by the much more efficient transmission of thermal energy from one point to another by the mobile electrons. Hence the well-known Wiedemann–Franz law that thermal and electrical conductivities of metals are proportional. Except at very low temperatures metals exhibit much higher thermal conductivities than dielectric solids. Metallic thermal conductivity decreases with temperature

because electrons are scattered by lattice vibrations. λ is also reduced by defects, such as are introduced by certain types of alloying. Figure 3.26 shows thermal conductivities of a variety of engineering materials, illustrating these general ideas.

Table 3.5 lists data for individual polymers. What emerges from a detailed study of such data may be summarised as follows.

(1) The range in λ found in solid polymers is small, all values lying within a factor of 2 of 0.22 $W m^{-1} K^{-1}$.

TABLE 3.5
Thermal properties of polymer materials

	Thermal linear expansivity ($10^{-5} K^{-1}$)	*Specific heat capacity* ($kJ kg^{-1} K^{-1}$)	*Thermal conductivity* ($W m^{-1} K^{-1}$)
PMMA	4.5	1.39	0.19
PS	6–8	1.20	0.16
PUR	10–20	1.76	0.31
PVC unplasticised	5–18.5	1.05	0.16
PVC 35% plasticiser	7–25	–	0.15
LDPE	13–20	1.90	0.35
HDPE	11–13	2.31	0.44
PP	6–10	1.93	0.24
POM copolymer	10	1.47	0.23
PA 6	6	1.60	0.31
PA 66	9	1.70	0.25
PETP	–	1.01	0.14
PTFE	10	1.05	0.27
PCTFE	5	0.92	0.14
EP	6	1.05	0.17
CR	24	1.70	0.21
NR	–	1.92	0.18
Fluorocarbon elastomer	16	1.66	0.23
Polyester elastomer	17–21	–	–
PIB	–	1.95	–
Polyethersulphone	5.5	1.12	0.18

Note: A comparison of published data on thermal properties shows numerous inconsistencies and uncertainties. The table contains selected values which should be regarded as indicative rather than firm.

(2) Crystalline polymers (PE, PP, PTFE, POM) show somewhat higher λ than amorphous polymers (PVC, PMMA, PS, EP).
(3) For most crystalline polymers, λ increases with density and crystallinity (for example, compare LDPE and HDPE).
(4) For amorphous polymers, λ increases with molar mass (that is, with chain length) because thermal energy flows more freely along polymer chains than between them. Similarly, addition of low molar mass plasticiser reduces λ for PVC.
(5) λ increases with temperature for some polymers, decreases for others. λ rarely changes by more than 10 per cent from 0 to 100 °C.
(6) The alignment of polymer chains by stretching produces an anisotropy in λ. λ for axial heat flow increases whereas for transverse flow it decreases. In the case of PVC at 300 per cent elongation, heat flows almost twice as rapidly along the axis as across it. High density PE exhibits a tenfold increase in λ along the axis of orientation at 1000 per cent strain. Similar effects have been observed in some rubbers.

Extremely low thermal conductivities can be achieved in cellular polymers; some representative data are given in table 3.6. For high and medium density foams, the thermal conductivity decreases as the density falls. λ is roughly the weighted mean of the thermal conductivity of solid polymer and blowing gas. λ of the foam may be significantly reduced by using a halocarbon gas

TABLE 3.6
Thermal conductivity λ of cellular polymer materials

	Density ($kg\ m^{-3}$)	λ ($W\ m^{-1}\ K^{-1}$)
PS	16	0.039
	25	0.035
	32	0.032
PVC	35	0.028
	45	0.035
UF	8	0.030
PUR	16	0.040
	32	0.023
	64	0.025
	96	0.043
PE	38	0.046

($\lambda = 0.009$ W m^{-1} K^{-1}) rather than air ($\lambda = 0.024$ W m^{-1} K^{-1}) for foaming. Such materials normally age as air diffuses slowly into the cells over weeks or months, causing the thermal conductivity to rise. In low density foams, heat transfer by convection and radiation becomes significant, and at the lowest densities (< 30 kg m^{-3}) the thermal conductivity once again rises.

Convection is only important in cells larger than about 5 mm in diameter. Radiative heat transfer was found to account for about 20 per cent of the total heat flow in a cellular PS at 30 °C. Both scattering and absorption (*see* chapter 5) of infrared radiation occur within the foam, and the rate of radiative heat transfer depends in a complicated way on cell size and polymer composition. Its importance increases rapidly as the temperature rises since the efficiency of radiative transfer increases approximately as T^2.

3.22 Specific Heat Capacity

Polymer data are given in table 3.5, and data for other engineering materials in table 3.7. c_p is determined largely by the chemical structure rather than the microstructure, and does not range widely among polymers. The amount of heat

TABLE 3.7
Specific heat capacity and expansivity of selected materials

	Thermal linear expansivity α ($K^{-1} \times 10^{-5}$)	*Specific heat capacity* c_p (kJ kg^{-1} K^{-1})
Brass	2.0	0.38
Carbon steel	1.1	0.48
Aluminium	2.3	0.88
Copper	1.7	0.38
Lead	2.9	0.13
Borosilicate glass	0.3	0.78
Building brick	0.5	0.8
Alumina	0.8	
Water	7 (liquid) 5 (ice)	4.2
Solid polymer materials	4–20	1–2

required to produce a particular rise in temperature depends on the vibrational and rotational motions excited within the solid. Replacement of hydrogen by heavier atoms such as F or Cl causes c_p to fall. Between the glass transition and melting temperature recrystallisation may occur, releasing heat from within the solid and making heating rates somewhat irregular.

3.23 Thermal Expansivity

Polymers as a class show higher expansivities than most metals and ceramics. The expansion of polymers is not usually a truly linear function of temperature (α is not constant). For example, the expansivity of PS increases rather erratically by about 50 per cent between 0 and 100 °C. The reason for differences in α between polymers has been little studied. However, engineering data are readily available. Changes in composition can produce significant changes in α. For example, the expansivity of epoxy resins is generally about 5×10^{-5} K^{-1}. Inorganic and metallic fillers can of course be incorporated to reduce α. The flexible formulations may show values as high as 20×10^{-5} K^{-1}. In some applications in which large temperature changes must be tolerated the designer may need to seek a compromise between modulus and expansivity to minimise thermal stresses.

3.24 Melting Range, Glass Transition Temperature and Softening Point

Semicrystalline polymers do not exhibit sharp melting points but fairly well defined melting ranges which may be measured by the methods of light microscopy, X-ray diffraction and scanning calorimetry. For both amorphous and crystalline polymers glass transition temperatures may be determined from changes in a variety of physical properties (*see* section 2.1). There exist also several simple standard test procedures to determine single-point properties of polymers such as the *heat distortion* or *deflection temperature* or the *softening point*. These are directly related to mechanical behaviour and have some limited comparative value.

3.25 Melt Properties

The mechanical properties of the polymer melt determine how easily a polymer may be melt processed (*see* chapter 6). High melt viscosities make extrusion and injection moulding difficult. The melt viscosity, measured by a rotating cylinder, rotating cone or capillary viscometer, is therefore a key indicator of 'processability': for polyolefins, the *melt flow index* is the standard measure, calculated from the mass of polymer which flows through a test orifice under specified load at a prescribed temperature.

While it is useful to talk of a simple melt viscosity, it would be very misleading to imply that molten polymers are rheologically simple. Detailed analysis of polymer melt flow (such as arises in the analysis of melt processing operations and tool design) has to take full account of their complex elastico-viscous properties. Just as polymer solids below T_m show creep and stress relaxation, so polymer melts show some elastic character. An important practical manifestation of this appears in the extrusion process. The reduction in compressive stress acting on the extruded polymer as it emerges from the die produces an increase in transverse dimensions: so-called *extrudate swell* or *die swell*. It is desirable to allow accurately for this elastic recovery in the design of extrusion dies.

Suggestions for Reading

Mechanical Properties

Aklonis, J. J. and MacKnight, W. J.; *Introduction to Polymer Viscoelasticity*, 2nd edn (Wiley–Interscience, New York, 1983).

American Society for Metals, *Polymeric Materials: Relationships between Structure and Mechanical Behaviour*, chs 4, 7 and 9 (ASM, Metals Park, Ohio, 1975).

Andrews, E. H., *Fracture in Polymers* (Oliver & Boyd, Edinburgh, 1968).

Andrews, E. H., 'Fracture', in A. D. Jenkins (Ed.), *Polymer Science: A Materials Science Handbook*, pp. 579–620 (North-Holland, Amsterdam, 1972).

Arridge, R. G. C., *An Introduction to Polymer Mechanics* (Taylor and Francis, London, 1985).

Bartenev, G. M. and Lavrentev, V. V., *Friction and Wear of Polymers* (Elsevier, Amsterdam, 1981).

Berry, J. P., 'Fracture of polymeric glasses', in H. Liebowitz (Ed.), *Fracture: An Advanced Treatise*, vol. 7, pp. 37–92 (Academic Press, New York, 1972).

Bowden, F. P. and Tabor, D., *Friction and Lubrication* (Methuen, London, 1967).

Briscoe, B. J. and Tabor, D., 'Friction and wear of polymers', in D. T. Clark and W. J. Feast (Eds), *Polymer Surfaces*, ch. 1 (Wiley, Chichester, 1978).

Brown, R. P., *Physical Testing of Rubbers* (Applied Science, London, 1979).

Brown, R. P. (Ed.), *Handbook of Plastics Test Methods*, 2nd edn (Godwin, London, 1981).

Bucknall, C. B., Gotham, K. V. and Vincent, P. I., 'Fracture – the empirical approach', in A. D. Jenkins (Ed.), *Polymer Science: A Materials Science Handbook*, pp. 621–685 (North-Holland, Amsterdam, 1972).

Cherry, B. W., *Polymer Surfaces* (Cambridge University Press, 1981).

Ferry, J. D., *Viscoelastic Properties of Polymers*, 2nd edn (Wiley, New York, 1970).

Hertzberg, R. W. and Manson, J. A., 'Fracture and fatigue', in *Encyclopaedia of Polymer Science and Engineering*, 2nd edn, vol. 8, pp. 328–453 (Wiley, New York, 1987).

Kambour, R. P., 'Crazing', in *Encyclopaedia of Polymer Science and Engineering*, vol. 4, pp. 299–323 (Wiley, New York, 1986).

Kambour, R. P. and Robertson, R. E., 'The mechanical properties of plastics', in A. D. Jenkins (Ed.), *Polymer Science: A Materials Science Handbook*, pp. 687–822 (North-Holland, Amsterdam, 1972).

Kinloch, A. J. and Young, R. J., *Fracture Behaviour of Polymers* (Applied Science, London, 1983).

Lancaster, J. K., 'Abrasion and wear', in *Encyclopaedia of Polymer Science and Engineering*, 2nd edn, vol. 1, pp. 1–35 (Wiley, New York, 1985).

Lee, L.-H. (Ed.), *Polymer Wear and its Control* (American Chemical Society, Washington DC, 1985).

Moore, D. F., *The Friction and Lubrication of Elastomers* (Pergamon, Oxford, 1972).

Moore, D. F., *Principles and Applications of Tribology* (Pergamon, Oxford, 1975).

Moore, D. F., *The Friction of Pneumatic Tyres* (Elsevier, Amsterdam, 1975).

Nielsen, L. E., *Mechanical Properties of Polymers and Composites*, 2 vols, (Dekker, New York, 1974).

Ogorkiewicz, R. M. (Ed.), *Engineering Properties of Thermoplastics* (Wiley-Interscience, London, 1970).

Pomeroy, C. D., (Ed.), *Creep of Engineering Materials* (Mechanical Engineering Publications, London, 1978).

Powell, P. C., *Engineering with Polymers* (Chapman and Hall, London, 1983).

Schultz, J. M., 'Fatigue behaviour of engineering polymers', *Treatise on Materials Science and Technology*, vol. 10 pt B, pp. 599–636 (Academic Press, New York, 1977).

Sternstein, S., 'Mechanical properties of glassy polymers' in J. M. Schultz (Ed.), *Treatise on Materials Science and Technology*, vol. 10, pt B, pp. 541–598 (Academic Press, New York, 1977).

Treloar, L. R. G., *The Physics of Rubber Elasticity*, 3rd edn (Oxford University Press, 1975).

Turner, S., *Mechanical Testing of Plastics*, 2nd edn (Godwin, London, 1984).

Vincent, P. I., *Impact Tests and Service Performance of Thermoplastics* (Plastics Institute, London, 1971).

Ward, I. M., *Mechanical Properties of Solid Polymers*, 2nd edn (Wiley-Interscience, London, 1983).

Ward, I. M., 'The preparation, structure and properties of ultra-high modulus flexible polymers', in *Advances in Polymer Science*, vol. 70, *Key Polymers – Properties and Performance*, pp. 1–70 (Springer, Berlin, 1985).

Ward, I. M., 'High modulus flexible polymers', in L. A. Kleintjens and P. J. Lemstra (Eds), *Integration of Fundamental Polymer Science and Technology* pp. 634–648 (Elsevier Applied Science, London, 1986).

Williams, J. G., 'Linear fracture mechanics', *Advances in Polymer Science*, 27 (1978) 67–120.

Williams, J. G., *Stress Analysis of Polymers*, 2nd edn (Longman, London, 1981)

Williams, J. G., *Fracture Mechanics of Polymers* (Ellis Horwood, Chichester, 1984).

Thermal Properties

Anderson, D. R. and Acton, R. U., 'Thermal properties', in *Encyclopaedia of Polymer Science and Technology*, vol. 13, pp. 764–788, (Wiley, New York, 1970).

Birley, A. W., and Couzens, D. C. F., 'Thermal properties', in R. M. Ogorkiewicz (Ed.), *Thermoplastics: Properties and Design*, ch. 8 (Wiley, London, 1974).

Brandrup, J. and Immergut, E. H. (Eds), *Polymer Handbook*, 2nd edn (Wiley, New York, 1975).

Hands, D., 'The thermal transport properties of polymers', *Rubber Chem. Technol.*, **50** (1977) 480–522.

Kline, D. E. and Hansen, D., 'Thermal conductivity of polymers', in P. E. Slade, Jr and L. T. Jenkins (Eds), *Thermal Characterization Techniques*, ch. 5 (Dekker, New York, 1970).